Apoptosis (2011) 16:1014–1027
DOI 10.1007/s10495-011-0625-x

ORIGINAL PAPER

Withaferin A induces apoptosis in human melanoma cells through generation of reactive oxygen species and down-regulation of Bcl-2

Eleonore Mayola · Cindy Gallerne · Davide Degli Esposti · Cecile Martel · Shazib Pervaiz · Lionel Larue · Brigitte Debuire · Antoinette Lemoine · Catherine Brenner · Christophe Lemaire

Published online: 28 June 2011

Abstract A high resistance and heterogeneous response to conventional anti-cancer chemotherapies characterize malignant cutaneous melanoma, the most aggressive and deadly form of skin cancer. Withaferin A (WFA), a withanolide derived from the medicinal plant *Withania somnifera*, has been reported for its anti-tumorigenic activity against various cancer cells. For the first time, we examined the death-inducing potential of WFA against a panel of four different human melanoma cells and investigated the cellular mechanisms involved. WFA induces apoptotic cell death with various IC_{50} ranging from 1.8 to 6.1 μM. The susceptibility of cells toward WFA-induced apoptosis correlated with low Bcl-2/Bax and Bcl-2/Bim ratios. In all cell lines, the apoptotic process triggered by WFA involves the mitochondrial pathway and was associated with Bcl-2 down regulation, Bax mitochondrial translocation, cytochrome *c* release into the cytosol, transmembrane potential ($\Delta\Psi m$) dissipation, caspase 9 and caspase 3 activation and DNA fragmentation. WFA cytotoxicity requires early reactive oxygen species (ROS) production and glutathione depletion, the inhibition of ROS increase by the antioxidant *N*-acetylcysteine resulting in complete suppression of mitochondrial and nuclear events. Altogether, these results support the therapeutic potential of WFA against human melanoma.

Keywords Melanoma resistance · Cell death · Oncogene · Chemotherapy

E. Mayola · C. Gallerne · C. Martel · C. Brenner · C. Lemaire (✉)
INSERM UMR S-769, Université Paris-Sud 11, 5 rue JB Clément, 92296 Châtenay-Malabry, France
e-mail: christophe.lemaire@uvsq.fr

E. Mayola · D. D. Esposti · C. Martel · B. Debuire · A. Lemoine
Faculté de Pharmacie, Châtenay-Malabry, INSERM U1004, Université Paris-Sud 11, Villejuif, France

E. Mayola · D. D. Esposti · C. Martel · L. Larue · B. Debuire · A. Lemoine · C. Brenner · C. Lemaire
PRES UniverSud Paris, Châtenay-Malabry, France

S. Pervaiz
Department of Physiology, Yong Loo Lin School of Medicine, National University of Singapore, Singapore, Singapore

L. Larue
Institut Curie, Université Paris-Sud 11, CNRS UMR3347/ INSERM U1021, Orsay, France

C. Lemaire
Université Versailles St-Quentin, Versailles, France

Introduction

Malignant cutaneous melanoma arising from melanocytes transformation is the most aggressive and deadly form of skin cancer. It has now become a public health issue since the incidence of this skin cancer increased more than 6-fold over the past 50 years and continues to rise worldwide [1]. One of the hallmarks of human melanoma is a high resistance and heterogeneous response to the chemo-, radio- and immuno-therapies available, the only cure remaining the total excision of the primary lesion [2]. Due to its high rate of progression, metastatic melanoma has poor prognosis, with a median survival estimated between 7 and 9 months [3]. Melanoma resistance to treatments has been reported to be, at least, promoted by high level of Bcl-2 family anti-apoptotic proteins (i.e. oncoproteins such as Bcl-2, Bcl-x_L and Mcl-1) and/or low expression of pro-apoptotic members (i.e. tumor suppressors such as Bax and Bak) [4]. A

high Bcl-2/Bax ratio was thus correlated with an unfavorable prognosis [5]. Accordingly, Bcl-2 antisense (e.g. Oblimersen) and small molecule mimetics of the pro-apoptotic BH3 domain (e.g. ABT737) are under intense preclinical and clinical investigation [4].

One critical hallmark of cancer cells is their resistance to apoptosis induction [6]. Therefore, inducing apoptosis is the aim of many anticancer therapeutic approaches as it enables to kill tumor cells without triggering inflammation [7]. Mitochondria are central to the intrinsic pathway of apoptosis and therefore are targets of choice for cancer therapy [8]. The mitochondrial pathway of apoptosis is characterized by mitochondrial membrane permeabilization (MMP) and release of pro-apoptotic proteins (e.g. cytochrome *c*) from the intermembrane space to the cytosol. These events launch activation of the initiator caspase 9, which in turn triggers the caspase cascade leading to DNA condensation/fragmentation and cell death [9]. MMP generally involves the formation of different types of pores, including Bax/Bak oligomers and the permeability transition pore complex (PTPC) [10]. The anti-apoptotic proteins Bcl-2 and Bcl-x_L can inhibit these pores and prevent apoptosis execution [10, 11].

Intracellular reactive oxygen species (ROS) may act as signaling molecules for carcinogenesis and cell death induction, a sudden intracellular raise in ROS accounting for a pro-death situation [12]. They are produced by various enzymatic complexes including NADPH oxidase and mitochondrial electron transport chain, the latter being considered as the most important source of ROS (in particular superoxide anion ($O_2^{\cdot -}$)) [13]. For instance, depending of their site of production, ROS can (i) directly modulate mitochondrial proteins such as VDAC, ANT as well as components of the oxidative phosphorylation to stimulate the MMP process or (ii) act as redox modifiers of enzyme function, inhibit the antioxidant cellular defenses and favor cell death. In comparison to melanocytes, melanoma cells were reported to present low antioxidant capacities, probably due to a down regulation of their antioxidant systems (including catalase, MnSOD and glutathione S-transferase) and to the loss of the scavenging function of melanin [14, 15]. Consequently, melanoma cells were suggested to be more sensitive to ROS-induced cell death than melanocytes [16], a vulnerability that can be exploited for the development of new anti-melanoma chemotherapeutics.

In recent years, natural products have received renewed interest in oncology for the discovery of new anticancer molecules. Withaferin A (WFA) is a bioactive withanolide extracted from the medicinal plant *Withania somnifera*, which has been safely used for centuries in Indian traditional medicine for its anti-inflammatory or antibacterial properties [17] and has recently been accepted as a dietary supplement in the United States. In addition, WFA has caught attention due to its cytotoxic properties demonstrated in a variety of human cancer cells including lymphoid leukemia [18–20], prostate [21, 22] and colon [23] cancers in vitro. The tumor cell inhibition activity of WFA has been proposed to rely on its anti-angiogenic properties [24] and its capacity to stimulate apoptosis [18–21, 25]. Although WFA inhibits Hsp90, NF-κB and proteasome [22, 26, 27], activates p38MAPK [19] and stimulates ROS production [18, 28], the pro-apoptotic cellular mechanisms of action of this withanolide are not fully understood.

In the present study we examined the apoptosis-inducing potential of WFA in a panel of different human melanoma cell lines and investigated the cellular pathways involved. We showed that WFA elicits apoptosis mediated through the mitochondrial pathway. This apoptotic process involves ROS-mediated activation of mitochondrial alterations and is dependent upon caspase activation. Our results also indicate that WFA decreases Bcl-2 expression and consequently that this promising natural molecule is able to overcome the endogenous apoptosis resistance of melanoma cells to cell death, even when anti-apoptotic Bcl-2 family members are highly expressed.

Materials and methods

Cell culture and reagents

Human cutaneous melanoma cell lines used throughout these experiments were: M14, originated from a metastatic nodule of human melanoma, Mel501, derived from human lymph nodes metastasis, SK28, obtained from a primary malignant melanoma and Lu1205, a metastatic variant of the WM793 cell line. M14 and Lu1205 cell lines were grown in DMEM: F12 and Mel501 and SK28 were maintained in RPMI 1640 at 37°C with 5% CO_2. All media were supplemented with 10% fetal bovine serum (FBS), 1% glutamax and 1% penicillin/streptomycin. Withaferin A (WFA) was purchased from Enzo Life Sciences and the pan-caspase inhibitor zVAD-fmk from Bachem. Unless specified, all others compounds were purchased from Sigma-Aldrich.

Assessment of cell viability, apoptosis and necrosis

Cell viability was studied using fluorescein diacetate assay (FDA). FDA is cleaved into fluorescein by intracellular esterases present in living cells. After treatments, cells were incubated for 10 min with FDA (1 μg/ml) at 37°C and analyzed by flow cytometry (Epics XL, Beckman Coulter). The type of cell death induced by WFA was determined by morphological analyses. Cells incubated for

24 h with WFA, were trypsinized, centrifuged and resuspended in PBS with 2 μM Hoechst to visualize DNA condensation/fragmentation. Immediately before observation, the impermeant probe propidium iodide (20 μg/ml) was added to determine early plasma membrane permeabilization associated with necrosis. Quantitative analyses were performed on a Leica fluorescence microscope (DMRH type) by counting more than 500 cells. To evaluate hypoploidy, SubG1 fractions were analyzed as described [29]. At least 10,000 cells were analyzed for each treatment.

Sample preparation for transmission electron microscopy

Cells were fixated with 4% glutaraldehyde/0.1 M sodium cacodylate for 1 h at room temperature (RT), pelleted and rinsed with 0.1 M sodium cacodylate/0.4 M sucrose for 1 h at RT. Samples were then paraffin-embedded, sliced, mounted on slides and the images were obtained at the electron microscopy facility of INRA (Jouy-en-Josas, France).

Analysis of DNA fragmentation in agarose gels

Cells (10^6) were trypsinized, washed with PBS and incubated 2 h at 50°C in lysis buffer (10 mM Tris-HCl, pH 7.4, 10 mM EDTA, 0.5% de SDS) containing 100 μg/ml proteinase K. The fraction containing low molecular weight DNA was isolated by centrifugation (15.000*g*, 15 min, 4°C) and precipitated with 70% cold ethanol. RNA was eliminated by incubation in RNase A buffer (10 mM Tris-HCl, pH 7.5, 1 mM EDTA, 1 μg/ml RNase A) for 1 h at 37°C and DNA fragments were precipitated with 70% cold ethanol. Electrophoresis of DNA fragments was performed in 1.2% agarose gels containing 100 μg/ml ethidium bromide.

Intracellular ROS and Glutathione measurement

The accumulation of mitochondrial superoxide anion ($O_2^{\cdot -}$) was determined with MitoSOX Red (Invitrogen). Cells treated with WFA were washed in HBSS 1× and stained with 2 μM MitoSOX Red at 37°C for 10 min. Intracellular hydrogen peroxide (H_2O_2) was measured using carboxy-H_2DFFDA probe (Invitrogen). Cells treated with WFA were washed with HBSS 1× and stained with 10 μM H_2DFFDA at 37°C for 10 min. Glutathione level was evaluated with the fluorescent probe monochlorobimane, as indicated by the manufacturer (Invitrogen). Fluorescence of cells was analyzed on Epics XL or Cell Lab Quanta MPL cytometers (Beckman Coulter).

Analysis of mitochondrial alterations

Mitochondrial transmembrane potential was assessed using the cationic dye $DiOC_6(3)$. Cells were incubated at 37°C with 100 nM of $DiOC_6(3)$ for 30 min and analyzed by flow cytometry. Inner mitochondrial membrane permeabilization was measured using calcein-AM/cobalt assay as previously described [29]. Briefly, cells were stained for 10 min at 37°C with calcein-AM (1 μM) in the presence of cobalt (1 mM) in Hank's balanced salt solution (HBSS, Invitrogen) supplemented with 1 mM HEPES. After staining, cells were treated with WFA. Calcein fluorescence was analyzed by flow cytometry. In each sample, at least 10,000 cells were analyzed.

Immunofluorescence

To determine intracellular localization of cytochrome *c* (cyt *c*), cells were seeded on slides in six-well multidishes, treated with WFA, washed in PBS 1×, fixed in 3.7% paraformaldehyde for 10 min at RT and permeabilized for 3 min in acetone at −20°C. Cells were saturated in PBS/3% bovine serum albumin (BSA) for 30 min and incubated for 1 h with anti-cyt *c* (mAb 6H2.B4, BD Biosciences) in PBS/1% BSA at RT. After two washes, the secondary antibody (Cy3-conjugated goat anti-mouse IgG, Jackson ImmunoResearch) was added in PBS/1% BSA. Nuclei were stained with 2.5 μg/ml Hoechst 33348 for 5 min. Micrographs were taken on a Leica fluorescence microscope.

Preparation of cytosolic and mitochondrial fractions

Mel501 cells (6 × 187.5 cm^2 flasks at 100% of confluence) were collected, washed in PBS, resuspended in buffer A (10 mM Tris-MOPS pH 7.4, 200 mM sucrose, 1 mM EGTA, 1 mg/ml BSA, 1 mM DTT) and lysed by Dounce homogenization. The suspension was centrifuged at 1.000*g* for 10 min at 4°C. The resulting supernatant was centrifuged at 15.000*g* for 15 min to pellet mitochondria. The cytosolic fraction (supernatant) was then obtained by centrifugation at 100.000*g* for 1 h at 4°C. Cytosolic proteins were precipitated with trichloroacteic acid (TCA) and solubilized in Laemmli sample buffer [30].

Mitochondria isolation

Mitochondria were isolated from 6 to 8 week old Balb/c mouse liver and purified on percoll gradient by centrifugation as previously described [30]. Mitochondria were also isolated from melanoma cells. Mel501 cells were harvested with trypsin/EDTA, centrifuged at 300*g* for 5 min, washed in PBS and resuspended in buffer A

(10 mM Tris-MOPS pH 7.4, 200 mM sucrose, 1 mM EGTA, 1 mg/ml BSA, 1 mM DTT). Cells were broken with a Dounce homogenizer (40 strokes) and suspension was centrifuged at 2.500*g* for 10 min at 4°C. The supernanatant was then centrifuged at 10.000*g* for 10 min at 4°C. The resulting pellet was washed and resuspended in buffer B (10 mM Tris-MOPS pH 7.4, 250 mM sucrose, 1 mM EGTA, 1 mg/ml BSA, 1 mM PMSF). Depolarization of Mel501 mitochondria was measured in hypo-osmotic buffer as for liver mitochondria.

Mitochondrial depolarization and swelling measurements

For depolarization and swelling measurements, mitochondria (25 μg protein) were diluted in a hypo-osmotic buffer (10 mM Tris-Mops, pH 7.4, 5 mM succinate, 300 mM sucrose, 1 mM Pi, 100 μM EGTA, 2 μM rotenone) and various doses of Ca^{2+}, CCCP, cyclosporin A (CsA) or WFA were added. Mitochondrial depolarization was measured by the rhodamine 123 (1 μM) fluorescence dequenching assay (λexc: 485 nm, λem: 535 nm, Invitrogen) at 37°C (Infinite M200, TECAN) and concomitantly, absorbance (540 nm) was recorded as a measure of the matrix swelling [31].

Western blot analysis

Cells were lysed in RIPA lysis buffer (50 mM Tris-HCl pH 8, 150 mM NaCl, 1% Triton, 1 mM EDTA, 0.1% SDS, 0.5% deoxycholic acid) plus a cocktail of protease inhibitors (Roche) and PMSF for 30 min at 4°C. Proteins (30 μg) were separated by SDS-polyacrylamide gel electrophoresis and transferred to PVDF membranes (Millipore). Membranes were incubated overnight at 4°C with the following antibodies: anti-caspase-9 (5B4) and anti-Mcl-1 (Y37) from Abcam, anti-caspase-3 and anti-Bcl-x_L (54H6) from Cell Signaling, anti-Bcl-2 (100), anti-Bax (N-20), anti-Bim (N-20) and anti-β-actin (C4) from Santa Cruz, anti-cytochrome c (7H8.2C12) from BD Bioscience and anti-VDAC (polyclonal serum, C. Brenner). Proteins were detected on a Chemidoc XRS (Biorad) by using the ECL method according to the manufacturer's instructions (Millipore).

Transfection experiments

Cells were transiently co-transfected with 1:5 ratio of pEGFP-N2 plasmid and either pcDNA3.1-V5 (empty vector) or pSFFV-Bcl-2 (kindly provided by Pr B. Mignotte, LGBC, Versailles, France [32]) vectors. Transfections were performed using ExGen 500 transfection reagent (Fermentas), according to the manufacturer's instructions. After 24 h of transfection, cells were incubated with WFA for another 24 h. To assess mitochondrial transmembrane potential, cells were stained with 100 nM CMXRos (Invitrogen) for 30 min a 37°C. The red fluorescence of CMXRos was determined by cytometric analysis of samples gated on GFP-positive cells.

Statistical analysis

Data obtained with cultured cells were analyzed using Student's t-test for all pair-wise comparisons of growth rates and mean responses to the different treatments tested. Results are presented as the mean ± SD for replicates experiments. Significance: $*P < 0.05$; $**P < 0.001$

Results

WFA induces apoptotic cell death in four human melanoma cell lines

We investigated the death-inducing potential of WFA (Fig. 1a) in four human melanoma cell lines (Lu1205, M14, Mel501 and SK28). Cells were incubated for 24 h with increasing concentrations of WFA and cytotoxicity was evaluated by flow cytometry. WFA induced a reduction of cell viability in a dose-dependent manner in all cell lines with a difference in the sensitivity according to the cell line studied (Fig. 1b). Indeed, the 24 h IC_{50} values were 1.8 ± 0.5 μM for Lu1205, 3.2 ± 1.8 μM for M14, 6.1 ± 0.4 μM for SK28 and 5.9 ± 0.2 μM for Mel501 cells. The type of cell death induced by WFA was then determined by dual staining of melanoma cells with Hoechst and propidium iodide (PI) (Fig. 1c). In the four cell lines, WFA induced apoptosis, the percentage of necrosis being very low and similar in controls and treated cells. Individual melanoma cell lines displayed differential sensitivity to 3 μM WFA, the percentage of apoptosis reaching 69.7 ± 5.5%, 47.9 ± 1%, 31.8 ± 4.3% and 23.3 ± 4.6% in Lu1205, M14, Mel501 and SK28 cell lines, respectively. Apoptosis was characterized further by analyzing cells morphology and DNA fragmentation. Cell morphological changes induced by WFA were assessed by transmission electron microscopy. In the absence of WFA (Fig. 1d), control cells presented a large cytoplasm and round-shaped nucleus. Following treatment with WFA, cytoplasm contraction and chromatin condensation were observed (Fig. 1e, black arrow). WFA treatment also induced DNA fragmentation (Fig. 1f, black arrow) and generation of apoptotic bodies. The characteristic pattern of apoptotic inter-nucleosomal DNA cleavage was visualized in response to WFA on agarose gel (Fig. 1g). This DNA

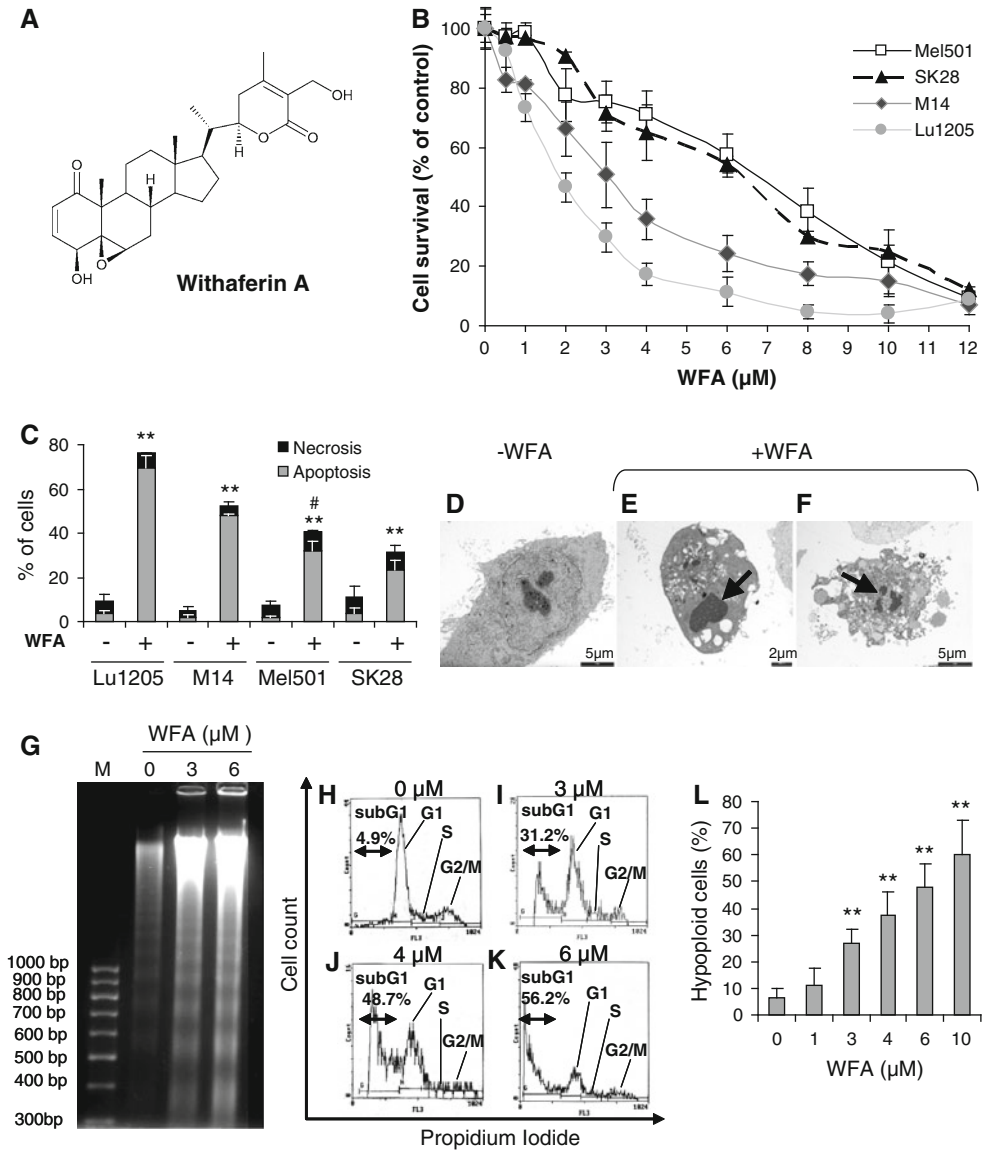

Fig. 1 WFA induces apoptosis in human melanoma cell lines. **a** Molecular structure of Withaferin A (WFA). **b** Effect of WFA on the viability of Lu1205, M14, Mel501 and SK28 cell lines. Cells were treated for 24 h with WFA at indicated doses, stained with fluorescein diacetate (FDA) and analyzed by flow cytometry. Results correspond to the mean ± SD of three independent experiments. **c** Quantification of apoptosis and necrosis in response to WFA. Cells treated with 3 μM of WFA were stained by the permeant dye Hoechst and the impermeant dye propidium iodide (PI) and more than 500 cells were counted on fluorescence microscope. Round and PI-stained nuclei were considered as necrotic, while fragmented or condensed nuclei were considered as apoptotic. Each *bar* represents means ± SD ($n = 3$). *$P < 0.05$. **d–f** Morphological changes induced by 3 μM WFA after 24 h of treatment. Non-treated (**d**) and treated (**e** and **f**) Mel501 cells were fixed, paraffin-embedded, sliced and mounted on slides. The electro-micrographs were obtained using a transmission electron microscope. *Black arrows* show condensed and fragmented nuclei. **g** WFA-induced internucleosomal DNA cleavage. After 48 h of treatment with 0, 3 and 6 μM of WFA, DNA of Mel501 cells was extracted and migrated on 1.5% agarose gel. M: 1 kb DNA Marker. **h–l** Quantification of the percentage of hypoploid cells (SubG1) induced by WFA. Mel501 were left untreated (**h**) or were treated for 48 h with 3 μM (**i**), 4 μM (**j**), 6 μM (**k**) or 0–10 μM (**l**) of WFA and DNA content was analyzed by flow cytometry. Each *bar* represents means ± SD ($n = 6$). *(apoptosis) or #(necrosis): $P < 0.05$; **$P < 0.001$

fragmentation was quantified by flow cytometry. WFA induced an increase in the percentage of hypoploid cells (subG1) in a dose-dependent manner starting at 4.9% in the control (Fig. 1h) and reaching 56.2% in the presence of 6 μM of WFA (Fig. 1k). The percentage of hypoploid cells induced by WFA showed a linear progression with increasing concentrations of WFA (Fig. 1l). Altogether, these results demonstrate that WFA triggers the morphological and nuclear changes characteristic of apoptosis in the four human melanoma cell lines tested.

WFA activates the mitochondrial pathway of apoptosis in melanoma cells

To assess the role of mitochondria in WFA-induced apoptosis, dose- and time-response studies were carried out. Upon WFA treatment, the four melanoma cell lines presented a decrease in $DiOC_6(3)$ fluorescence, demonstrating a loss of $\Delta\Psi m$ in a dose-dependent (Fig. 2a) and time-dependent manner (Fig. 2b). Mitochondrial membrane depolarization occurred at 1 μM WFA in Lu1205 and M14 cell lines (with 26.5 ± 9.9% and 38.3 ± 6.6% of cells with dissipated $\Delta\Psi m$ respectively), whereas no loss of $\Delta\Psi m$ was observed in Mel501 and SK28 cell lines at this concentration. Moreover, the earlier $\Delta\Psi m$ disruption occurred in Lu1205 cell line between 6 and 16 h of incubation with 3 μM of WFA. WFA being associated with mitochondrial membrane depolarization, its ability to promote inner mitochondrial membrane (IMM) permeabilization was next investigated using the calcein/cobalt assay [29, 33]. As shown in Fig. 2c, WFA induced an increase in the percentage of cells with low calcein fluorescence (calcein low) in the four melanoma cell lines with values ranging between 75.6 ± 16.1% for Lu1205 to 40.4 ± 13.8% for SK28 cell lines. These results demonstrated that loss of $\Delta\Psi m$ is associated with IMM permeabilization.

We then questioned whether WFA would directly target the mitochondrion. To this end, we performed in vitro assays on mouse liver purified mitochondria. Kinetics of the effect of WFA on mitochondrial matrix swelling (Fig. 2d, e) and $\Delta\Psi m$ dissipation (Fig. 2f, g) were concomitantly recorded. When treated with the permeability transition inducer calcium (Ca^{2+}), isolated mitochondria underwent dose-dependent swelling (Fig. 2d) and loss of $\Delta\Psi m$ (Fig. 2f). These mitochondrial events were mediated by the opening of PTPC since they are totally inhibited by

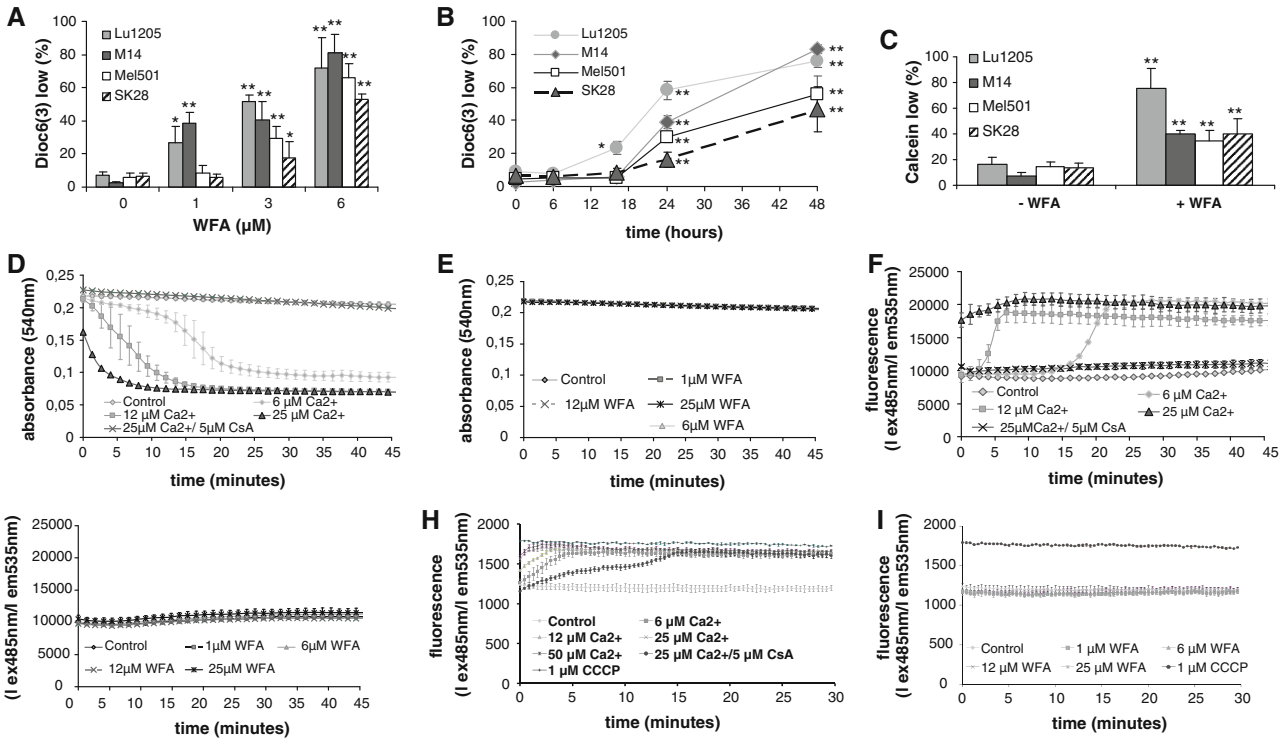

Fig. 2 WFA induces the mitochondrial events of apoptosis in human melanoma cell lines **a**, **b** Effect of WFA on mitochondrial membrane potential ($\Delta\Psi m$). **a** Dose–response of WFA on $\Delta\Psi m$. Cells were treated for 24 h with the indicated doses of WFA, stained with $DiOC_6(3)$ dye and analyzed by flow cytometry. Each *bar* represents means ± SD ($n = 6$). **b** Kinetics of WFA effect on $\Delta\Psi m$. Cells were incubated with 3 μM of WFA for the indicated time, stained with $DiOC_6(3)$ and analyzed by flow cytometry. Each value represents means ± SD ($n = 3$). **c** Effect of WFA on inner mitochondrial membrane permeabilization. Cells were stained with calcein and cobalt, treated with 3 μM of WFA for 24 h and calcein fluorescence was quantified by flow cytometry. Each *bar* represents means ± SD ($n = 6$). **d**–**g** Effect of WFA on purified mitochondria. Mitochondria were isolated from mouse liver and kinetics of matrix swelling (A540 nm) and dissipation of $\Delta\Psi m$ (Rhod123 fluorescence) were recorded in response to calcium and WFA. As a positive control mitochondria were incubated with different doses of calcium. Cyclosporine A (CsA, 5 μM), an inhibitor of PTPC, was used to inhibit mitochondrial alterations. To determine the effect of WFA, mitochondria were incubated with various concentrations of this drug (1, 6, 12 and 25 μM) and matrix swelling (**e**) and drop of $\Delta\Psi m$ (**g**) were recorded for 45 min. No effect of WFA on purified mitochondria was observed ($n = 5$). **h**–**i** Dissipation of $\Delta\Psi m$ was also recorded in mitochondria isolated from Mel501 cells in response to Ca^{2+}, CCCP and WFA ($n = 3$). $^*P < 0.05$; $^{**}P < 0.001$

cyclosporin A (CsA), a well-known inhibitor of this pore. By contrast, neither ΔΨm dissipation nor matrix swelling was observed in response to concentration of WFA ranging from 1 to 25 μM (Fig. 2e, g). These results were confirmed with mitochondria isolated from Mel501 cells (Fig. 2h, i). Therefore, WFA does not appear to directly target the mitochondrion or the PTPC, but rather acts at an upstream step to activate the mitochondrial pathway of apoptosis.

By definition, upon MMP, mitochondria release apoptogenic factors such as cytochrome c (Cyt *c*) from the intermembrane space to the cytosol [10]. The subcellular localization of Cyt *c* was thus investigated in response to

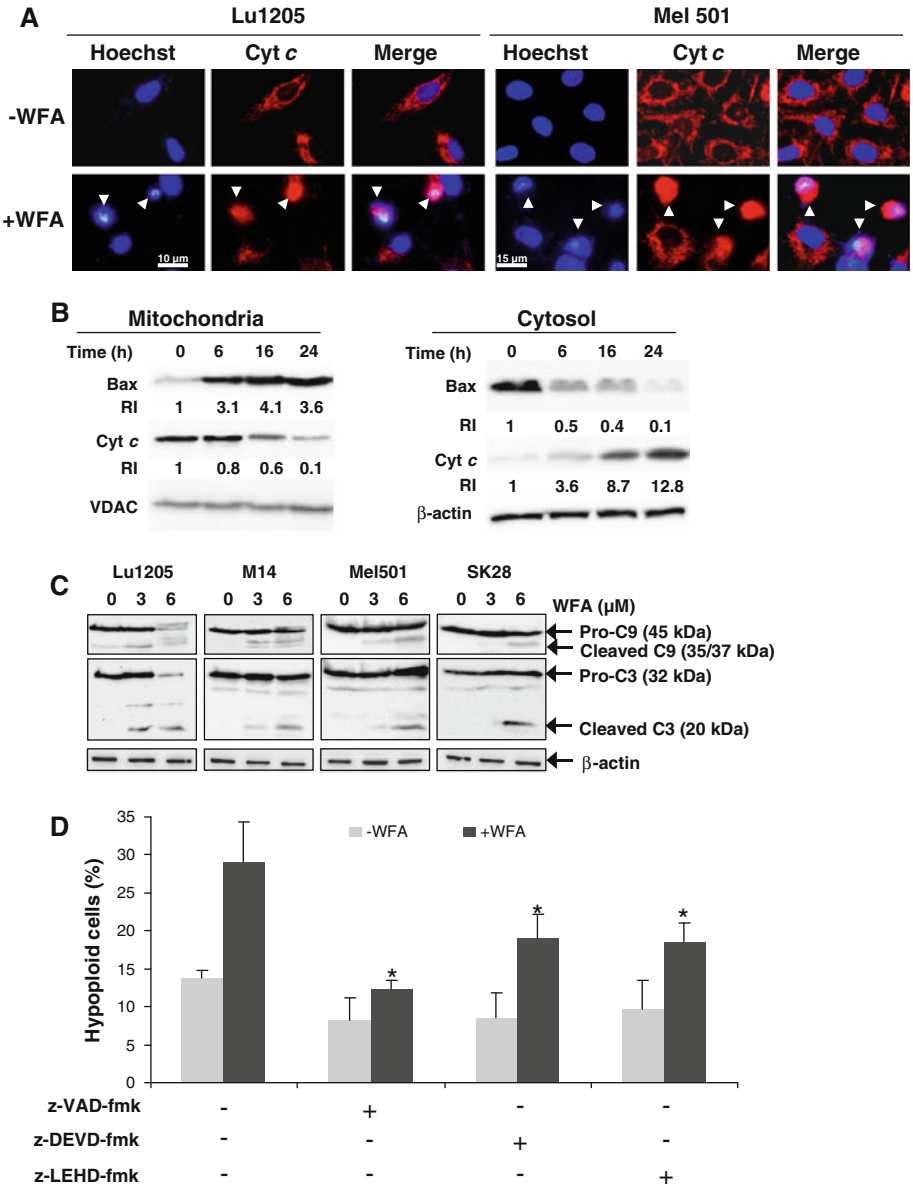

Fig. 3 WFA induces Bax translocation, cytochrome *c* release and caspase activation. **a** Release of the apoptogenic protein cytochrome *c* (Cyt *c*) from the intermembrane space to the cytosol following WFA treatment. Lu1205 and Mel501 cells were left untreated (−WFA) or were treated with 3 μM of WFA for 16 h (+WFA) and Cyt *c* localization was assessed by immunofluorescence using anti-Cyt *c* antibody combined with Hoechst staining to assess nuclear morphology (Hoechst). Arrows indicate cells with a cytoplasmic Cyt *c* localization and condensed nuclei. **b** Time course study of protein subcellular localization. Cells treated with WFA for various period of time were fractionated by centrifugation to separate mitochondria and cytosol. Proteins were separated by SDS-PAGE and immunoblotted for Cyt *c*, Bax, VDAC and *β*-actin. *RI* relative intensity. **c** WFA treatment induced caspases-9 and -3 cleavage. Cells were treated for 16 h with WFA (0, 3 and 6 μM) and analyzed by western-blot using anti-caspase-9 and -3 antibodies. Caspases-9 and -3 pro-forms (Pro-C9 and Pro-C3) of respectively 45 and 32 kDa were cleaved into their 37/35 and 20 kDa active forms following WFA treatment. **d** Effect of caspase inhibitors on WFA-triggered apoptosis. Lu1205 and SK28 cells were incubated with 50 μM of z-VAD-fmk, 75 μM of z-DEVD-fmk, or 75 μM of z-LEHD-fmk for 1 h prior to WFA treatment (3 μM, 24 h) and the percentage of hypoploid cells were recorded by flow cytometry. $*P < 0.05$. Each *bar* represents means ± SD of three separate experiments

WFA by immunofluorescence analysis (Fig. 3a) and cell fractionation (Fig. 3b). Following WFA exposure, the subcellular distribution of Cyt *c* shifted from punctuate to diffuse staining pattern in apoptotic cells with fragmented nucleus upon treatment with WFA, indicating relocalization of Cyt *c* from the mitochondrial intermembrane space to the cytosol. The time-course study of Cyt *c* redistribution shows that the release occurred from 6 h of treatment and is maximal at 24 h (Fig. 3b). Moreover, this release is concomitant with the translocation of Bax from the cytosol to the mitochondrial compartment, suggesting the involvement of Bax in the permeabilization of outer mitochondrial membrane (Fig. 3b). The caspase cascade has been demonstrated to be activated downstream of the mitochondrion by Cyt *c* release and apoptosome formation in the presence of ATP [34]. We therefore wondered whether WFA would trigger a caspase-dependent apoptosis in human melanoma cells. Western-blot experiments shown in Fig. 3c indicate that in response to WFA, caspase-9 and caspase-3 proforms (Pro-C9 and Pro-C3) were cleaved to their active products in the four cell lines tested. To test whether caspase activity is required for WFA-induced apoptosis, cells were pre-treated with various caspase inhibitor followed by 24 h treatment with or without 3 μM WFA. Pre-incubation with z-VAD-fmk, a pan caspase inhibitor, strongly inhibited the WFA-induced nuclear events of apoptosis (Fig. 3d). Z-DEVD-fmk and z-LEHD-fmk, inhibitors of caspase 3 and 9, respectively, also inhibited significantly the death induced by WFA, suggesting the implication of both effector caspases in the process but also that other caspase(s) may be required for the cell death. These results indicate that WFA triggered several hallmarks of pro-apoptotic mitochondrial membrane permeabilization, such as Bax translocation and Cyt *c* release, leading subsequently to caspase-dependent nuclear alterations.

Reactive oxygen species elevation is an early and critical event in WFA-induced apoptosis in melanoma cells

ROS, such as hydrogen peroxide (H_2O_2) and anion superoxide ($O_2^{\cdot -}$), have been involved in cell death regulation [35, 36]. We therefore examined the prooxidant potential of WFA in melanoma cells. Mitochondrial accumulation of $O_2^{\cdot -}$ was investigated using MitoSOX red dye, which is targeted to mitochondria and was reported to be preferentially oxidized by $O_2^{\cdot -}$ [37]. The generation of intracellular H_2O_2 was measured using the cell permeant non fluorescent molecule H_2DFFDA. This probe becomes fluorescent when oxidized in difluorofluorescein (DFF) by H_2O_2 and its free radical products [38]. In all cell lines, an increase in the percentage of cells with elevated MitoSOX (MitoSOX high) and DFF fluorescence (DFF high) was observed, indicating mitochondrial $O_2^{\cdot -}$ and intracellular H_2O_2 production in response to WFA treatment (Fig. 4). The percentages of MitoSOX high cells were about 2- to 5-fold higher than in controls and the percentages of DFF high cells were 1.5- to 7-fold increased compared to controls depending on the cell line. Unexpectedly, in SK28 cell line, which is more resistant to WFA-induced apoptosis, the basal rate of H_2O_2 was about 3- or 4-fold higher than in other cell lines. To determine whether ROS production is upstream or downstream of mitochondrial alterations, cells were pre-incubated for 1 h with the antioxidant molecule *N*-acetylcysteine (NAC), a thiol antioxidant, which functions as both redox buffer and ROS scavenger [39]. NAC totally inhibited intracellular H_2O_2 and mitochondrial $O_2^{\cdot -}$ accumulation induced by WFA. We further examined whether the abrogation of intracellular and mitochondrial ROS by NAC could inhibit all downstream events of WFA-induced apoptosis. Cells were pre-treated with NAC, incubated with WFA and dissipation of $\Delta\Psi m$ ($DiOC_6(3)$ low cells) and IMM permeabilization (calcein low cells) were analyzed by flow cytometry (Fig. 5a). In Lu1205 cell line, pre-incubation with NAC markedly reduced the loss of $\Delta\Psi m$ (67.9 ± 11.1% in WFA alone vs. 25.5 ± 10.3% in WFA + NAC) and IMM permeabilization (63.5 ± 15.5% in WFA alone vs. 22.7 ± 10.2% in WFA + NAC) triggered by WFA. In all the other cell lines (M14, Mel501 and SK28), the mitochondrial alterations induced by WFA were completely prevented by NAC. We then questioned if the nuclear events provoked by WFA could occur in the absence of ROS production. As shown in Fig. 5b, pre-treatment with NAC also totally preserved cells from nuclear apoptotic changes triggered by WFA. Altogether, these results show that ROS elevation is crucial for WFA-induced melanoma apoptosis. Prompted by the observation that NAC protects from WFA-induced apoptosis, we evaluated the content of intracellular glutathione (GSH) [40], the principal intracellular low-molecular-weight thiol, which plays a critical role in the cellular defense. Thus, to determine whether WFA can affect a detoxifying enzyme, namely the glutathione S-transferase, we used monochlorobimane (MCB), a thiol binding dye [41], and observed a dose-dependent loss of GSH during WFA, indicating that the enzyme is not profoundly affected directly by WFA (Fig. 4b–c).

Bcl-2/Bax and Bcl-2/Bim ratios are important determinants of the sensitivity of melanoma cells to WFA

As presented in cell survival assay (Fig. 1b), cell death quantification (Fig. 1c) and $\Delta\Psi m$ analyses (Fig. 2a), the four melanoma cell lines used in our study displayed

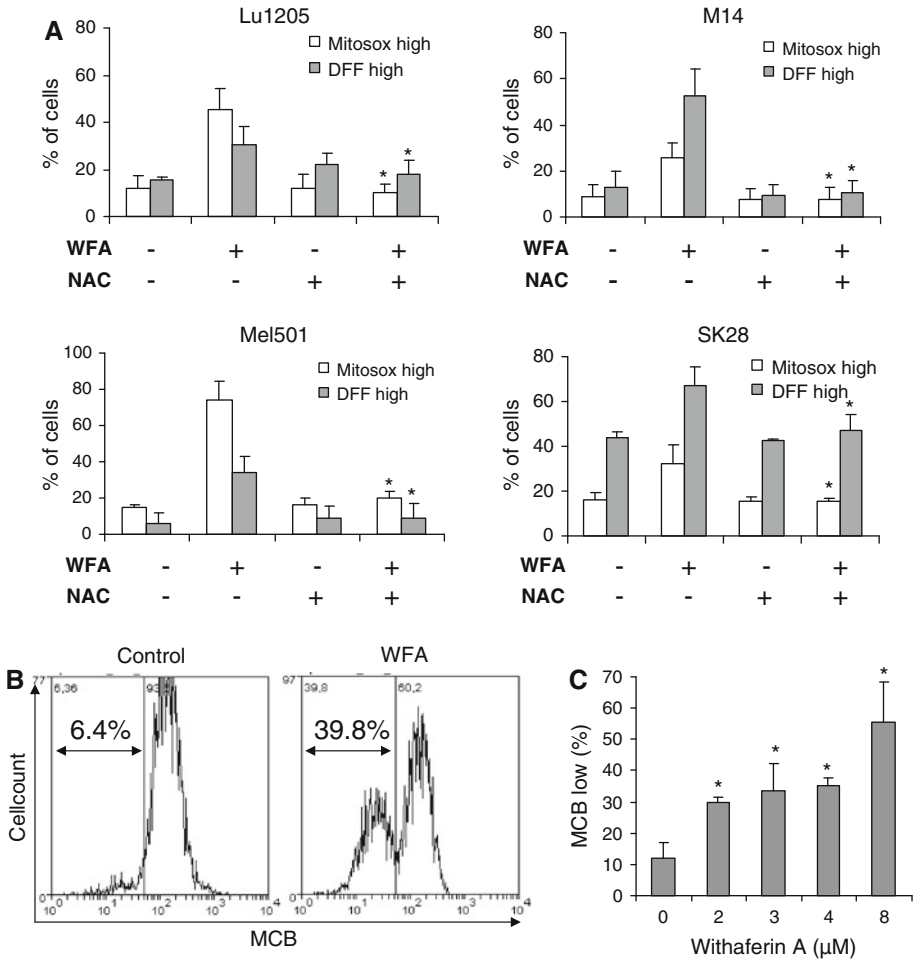

Fig. 4 WFA induces *N*-acetylcysteine-inhibitable ROS production. Mitochondrial superoxide anion (O_2^-) and cellular hydrogen peroxide (H_2O_2) accumulation induced by WFA treatment. Cells treated with 3 μM WFA for 24 h were stained with MitoSOX Red dye (2 μM) to quantify mitochondrial O_2^- or with H2DFFHDA probe (10 μM) to measure cellular H_2O_2. Fluorescence of the probes was quantified by flow cytometry. When indicated, pre-incubation of 1 h with the antioxidant *N*-acetylcysteine (NAC, 5 mM) was done. Each *bar* represents means ± SD of four separate experiments. MitoSOX high: cells with high MitoSOX fluorescence presenting mitochondrial O_2^- accumulation. DFF high: cells with high DFF fluorescence presenting cellular H_2O_2 generation. **b–c** Glutathione (GSH) content determination. Changes in GSH were determined by flow cytometry using the thiol binding dye monochlorobimane (MCB). For the induction of apoptosis, Mel501 cells were incubated with various concentrations of WFA for 24 h. $^*P < 0.05$

different susceptibilities towards WFA. Lu1205 and M14 cell lines appeared qualitatively more sensitive than Mel501 and SK28 to WFA-induced apoptosis. Therefore, we investigated the possible causes of this difference. A strategy for melanoma and other cancer cells to resist to cell death is to express multidrug resistance (MDR) proteins, membrane transporters that facilitate the efflux of drugs out of the cells [42]. We thus investigated whether the MDR transporters were involved in Mel501 and SK28 resistance to WFA by using MDR inhibitor LY335979 that has been shown to reverse MDR-induced resistance [43]. When cells were pre-incubated with LY335979, no difference in WFA-induced apoptosis of Mel501 and SK28 was observed (data not shown), suggesting that the less susceptibility of these two cell lines is not due to MDR up-regulation.

In melanoma, anti-apoptotic proteins such Bcl-2, Bcl-x_L and Mcl-1 are highly expressed [4, 44] and resistance to apoptosis has been correlated to high Bcl-2/Bax ratio [5]. We thus investigated whether Bcl-2 family proteins could account for the difference of response of melanoma cell lines to WFA. The basal levels of Mcl-1, Bcl-x_L, Bcl-2, Bax and Bim were thus compared by western blot in all cell lines in the absence of treatment. As observed in Fig. 6a, M14 and Lu1205 presented a higher basal level of Mcl-1 compared to Mel501 and SK28. The level of Bcl-x_L was elevated in both M14 and Mel501 cells (Fig. 6b). Interestingly, the highest levels of Bcl-2 (Fig. 6c) were observed in Mel501 and SK28

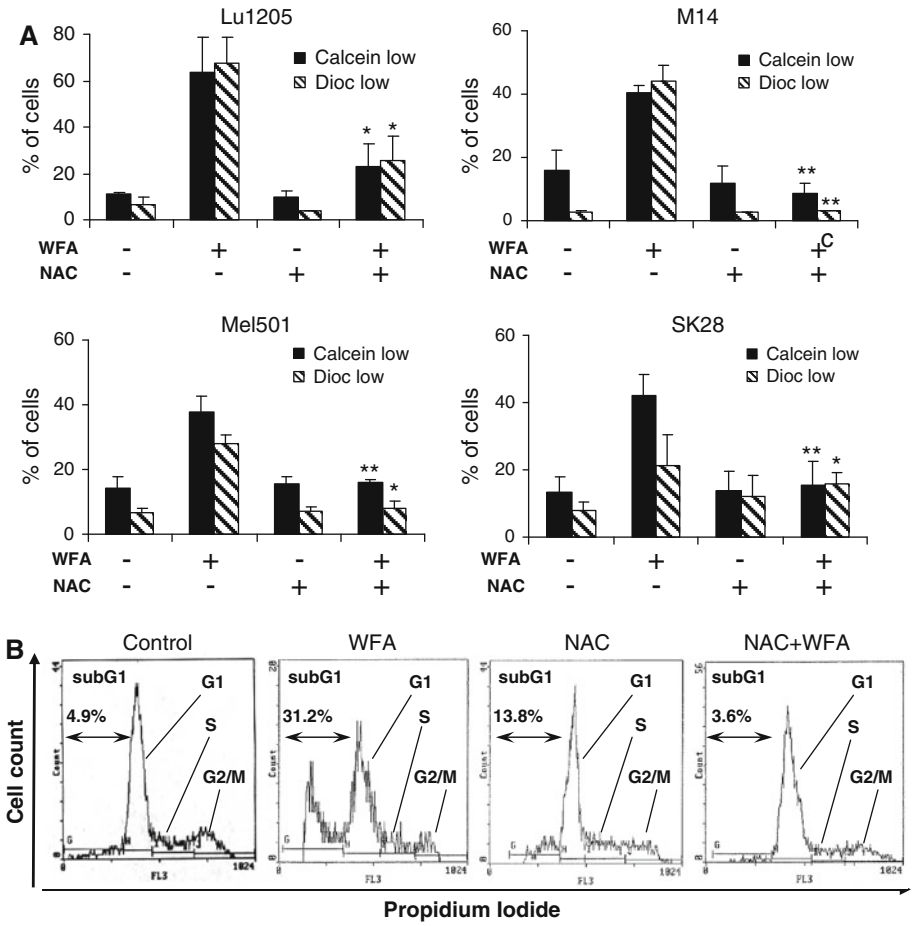

Fig. 5 NAC inhibits mitochondrial and nuclear alterations induced by WFA. **a** Inhibition of WFA-triggered mitochondrial events by NAC. Cells pre-incubated or not for 1 h with 5 mM NAC were treated for 24 h with 3 μM WFA, stained with $DiOC_6(3)$ or calcein/cobalt and analyzed by flow cytometry. Dioc low: cells with low $\Delta\Psi m$. Calcein low: cells presenting IMM permeabilization. Each *bar* represents means ± SD ($n = 6$). **b** Inhibition of WFA-induced nuclear apoptotic events by NAC. Mel501 cells were pre-incubated or not with 5 mM NAC and treated with 3 μM WFA for 48 h. Hypoploid cells (subG1) were quantified by flow cytometry as described previously. * $P < 0.05$; ** $P < 0.001$

compared to M14 and Lu1205, suggesting a correlation between Bcl-2 expression and susceptibility of cells towards WFA. For instance, in less sensitive Mel501 cells, the level of Bcl-2 was 2.3-fold higher than in Lu1205 and 6.8-fold higher than in M14. Of note, the cell lines expressing the highest level of Bcl-2 also showed the lowest level of Mcl-1. The expression of endogenous pro-apoptotic protein Bax (Fig. 6d) was found higher in M14 than in the other cell lines, while the pro-apoptotic protein Bim was more expressed in Lu1205 (Fig. 6e). Anti-apoptotic over pro-apoptotic proteins ratios being associated with chemoresistance, we measured the ratio of Mcl-1/Bim, Bcl-x_L/Bax, Bcl-2/Bax and Bcl-2/Bim ratios (Fig. 6f). The Mcl-1/Bim ratio and Bcl-x_L/Bax ratio did not appear to determine the proneness of melanoma cells to WFA-induced apoptosis. Regarding Bcl-2/Bax ratio, Lu1205 and M14 cells presented the lowest values (0.46 and 0.09, respectively), while in the less responsive Mel501 and SK28 cell lines the Bcl-2/Bax ratio was much higher (0.88 et 0.87, respectively). Similarly, low Bcl-2/Bim ratio correlates with a higher sensitivity of Lu1205 cells (0.42) and M14 cells (0.23) compared to SK28 cells (1.43) and to Mel501 (1.32). Our results therefore suggest that a low Bcl-2/Bax ratio as well as low Bcl-2/Bim correlate with a higher sensitivity to WFA.

WFA induces mitochondrial alteration via a down-regulation of Bcl-2 protein level

In order to better define the involvement of Bcl-2 in the regulation of WFA-activated apoptotic signaling pathway, we explored the mitochondrial effect of WFA in melanoma cells. To that end, Mel501 cells were transfected with a pSFFV-Bcl-2 plasmid encoding Bcl-2 or with the empty plasmid (Fig. 6g). Thus, Bcl-2 overexpressing cells appeared resistant to WFA treatment as the percentage of cells with dissipated $\Delta\Psi m$ was markedly reduced from 70.7 ± 0.4% to 52.9 ± 0.1%, indicating the capacity of Bcl-2 to prevent significant WFA-induced mitochondrial dysfunction and then, to stabilize the mitochondrial membrane integrity. We next investigated the effect of WFA on Bcl-2 expression in the four melanoma cell lines. As depicted in Fig. 6h, the level of Bcl-2 was down-regulated in response to WFA in all cell lines from 35 to 80% compared to controls, suggesting an effect of WFA on the transcription or on the degradation of Bcl-2. In addition, the more important decrease of Bcl-2 level was observed in the more sensitive M14 and Lu1205 cell lines to WFA treatment. Of note, the decrease in Bcl-2 protein was found concomitantly with

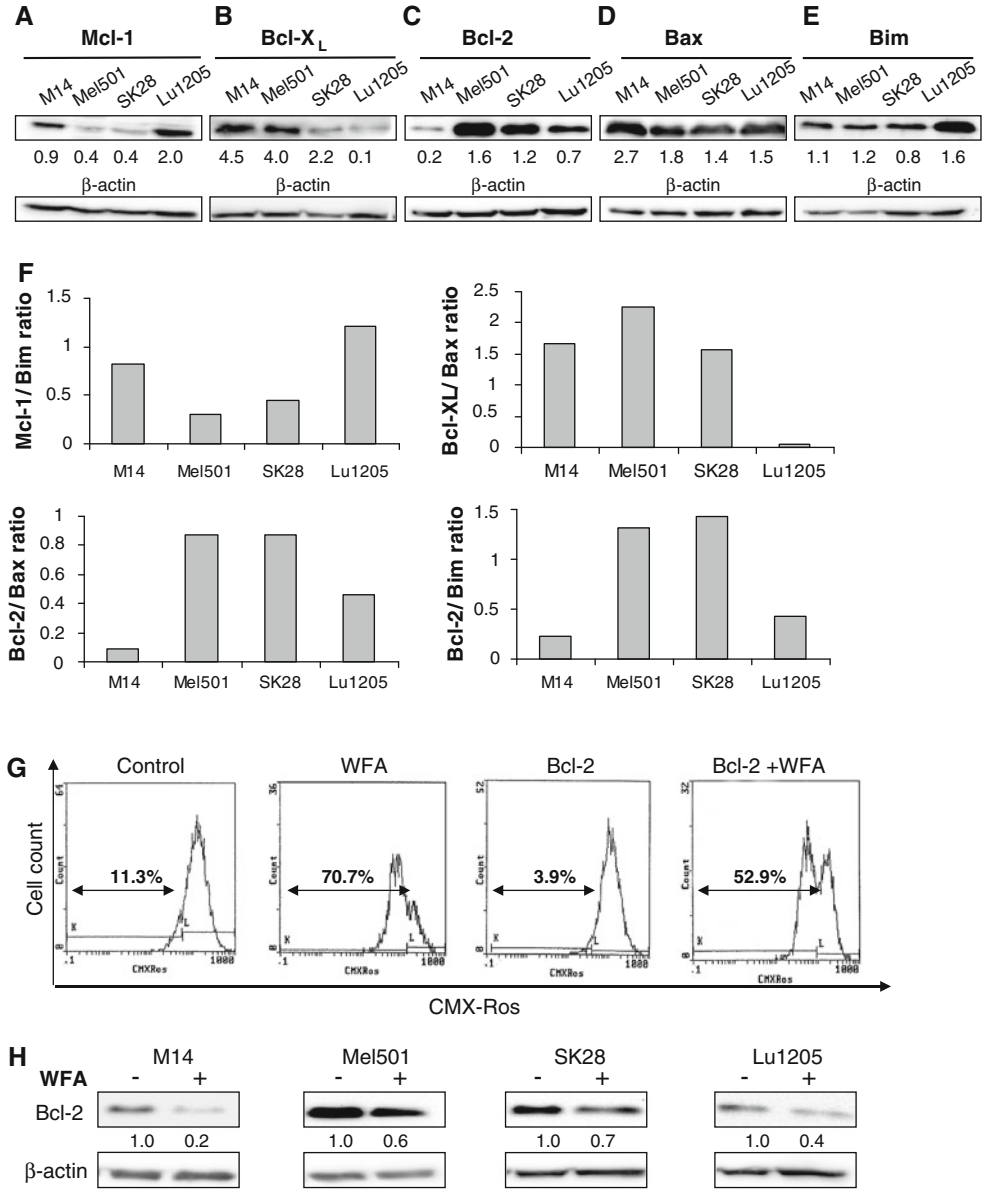

Fig. 6 Bcl-2/Bax and Bcl-2/Bim ratios correlate with human melanoma cells sensitivity towards WFA and WFA decreases Bcl-2 expression. Constitutive level of the anti-apoptotic proteins Mcl-1 (**a**), Bcl-x_L (**b**) and Bcl-2 (**c**), and of the pro-apoptotic proteins Bax (**d**) and Bim (**e**). Cell lysates were subjected to western blot using the indicated antibodies. Optical densities (OD) were determined using ImageJ analysis software. For each protein, the OD obtained was normalized to the OD of *β*-actin and reported on bottom of immunoreactive bands. **f** The expression ratios of Mcl-1/Bim, Bcl-x_L/Bax Bcl-2/Bax and Bcl-2/Bim were calculated and presented on the graphs. **g** Bcl-2 overexpression only slightly prevents ΔΨm loss induced by WFA treatment. Mel501 were co-transfected with plasmids encoding GFP and either pcDNA3.1 (Control and WFA) or Bcl-2 (Bcl-2 and Bcl-2 + WFA) for 24 h prior to treatment with 3 μM WFA for another 24 h. Drop of ΔΨm was assessed by CMX-Ros staining in the GFP positive cell population by flow cytometry ($n = 3$). **h** WFA down-regulates Bcl-2 protein level. Cells were incubated in the absence (−WFA) or the presence (+WFA) of 3 μM WFA for 24 h and the level of Bcl-2 was evaluated by western blot. The results are expressed as the percent of the level of Bcl-2 in the absence of treatment. Results are representative of three independent experiments

the loss of ΔΨm following 24 h of treatment. Altogether, these data demonstrate that this drug kills human melanoma cells via its ability to decrease the level of this anti-apoptotic protein which prevents mitochondrial membrane permeabilization.

Discussion

The objectives of the present study were to investigate the death-inducing potential of the natural compound Withaferin A (WFA) against human melanoma cells and to

decipher the cellular mechanisms involved. To the best of our knowledge, we demonstrated here for the first time that WFA induces cell death in several human melanoma cell lines and described the hierarchy of the lethal events involved. Our results show that exposure of four different human melanoma cell lines to micromolar concentrations of WFA enables apoptotic cell death as evidence by nuclear condensation and fragmentation, inter-nucleosomal DNA cleavage, hypoploid cell accumulation and formation of apoptotic bodies. This apoptotic process involved the activation of the mitochondrial pathway and is sequentially associated with ROS production, GSH depletion, Bax translocation, Cyt *c* release, Bcl-2 down-regulation, loss of $\Delta\Psi m$, caspase 3 and 9 activation, and nuclear fragmentation.

Intracellular ROS generation induced by WFA appears to be an upstream event of the apoptotic cascade since mitochondrial and nuclear alterations are fully inhibited by the antioxidant NAC (Fig. 4, 5). Thus, even if WFA may have the ability to activate several different pathways that converge to the apoptotic cell death, ROS are the earliest event that we identified before any other hallmarks of apoptosis. The ability of WFA to induce early generation of ROS and subsequent apoptosis was also observed in HL60 leukemia cells [18], showing also the importance of the pro-oxidant activity of WFA. Although the MitoSOX probe led us to demonstrate a mitochondrial accumulation of $O_2^{\cdot -}$, the cellular origin of ROS production triggered by WFA was not precisely determined in our study. Indeed, superoxide anion has been reported to be mainly produce by NADPH oxidase of the plasma membrane (NOX, [45]), xanthine oxidase into the cytosol, and the mitochondrial respiratory electron transport chain [46]. WFA may thus stimulate $O_2^{\cdot -}$ production by activating NOX or by inhibiting complex I or complex III of the electron transport chain (ETC). Nevertheless, no effect of WFA was found on purified mitochondria, even at high concentrations, suggesting that WFA would rather activate production of ROS upstream of the mitochondrion or inhibit detoxifying enzymes such as thioredoxin or glutathione peroxidase. In cellulo, the accumulation of these ROS is known to result in MMP and dissipation of $\Delta\Psi m$ [12, 47]. It has been shown that melanoma cells present a decrease in antioxidant capacities compared to melanocytes [14]. Therefore, WFA, by inducing both a strong rise in intracellular ROS and GSH depletion may take advantage of the low antioxidant system of melanoma cells to induce a high rate of apoptosis. This prooxidant activity of WFA is of great interest in the development of new treatments against human melanoma [48] since other ROS-inducing agents, including menadione and disulfiram, are currently being tested in combination with other agents in clinical trials on patients with metastatic melanoma (ClinicalTrials.gov identifiers: NCT01001299 and NCT00571116). Interestingly, the SK28 cell line showed the higher steady state level of H_2O_2 and presented the lowest increase of this ROS following WFA treatment (Fig. 4). This cell line, which is more resistant to apoptosis induction, may possess a more efficient antioxidant system than the others, allowing it to survive a particularly high H_2O_2 rate and enabling it to be more resistant to prooxidant treatment. WFA could thus be more efficient if associated with other molecules known to weaken the antioxidant system. For example, buthionine sulfoximine is known to deplete the pool of glutathione in cells [49] and is in clinical trial in association with melphalan to treat patients with persistent malignant melanoma (ClinicalTrials.gov identifier: NCT00661336).

Although the anti-apoptotic proteins Bcl-2, Bcl-x_L and Mcl-1 appear of particular importance in melanoma chemoresistance, their respective role in metastasized melanoma resistance remains unclear [4]. To better understand the contribution of these proteins in sensitivity of human melanoma to WFA-induced apoptosis, we compared their constitutive expression level. No apparent correlation was found between expression of Mcl-1 or Bcl-x_L and the sensitivity of cells toward WFA. In contrast, Bcl-2 is constitutively more abundant in the less sensitive cell lines Mel501 and SK28 than in M14 and Lu1205, suggesting a correlation between expression of Bcl-2 and sensitivity of melanoma cells to WFA treatment. Nevertheless, the susceptibility of cancer cells to chemotherapy has been shown to be influenced by the relative ratios of the various pro- and anti-apoptotic proteins of Bcl-2 family rather than by the expression of only one member of this family. Bcl-2 and Bcl-x_L have been shown to prevent Bax activation [4], while Mcl-1 was found in complex with Bim thus inhibiting its pro-apoptotic activity [50]. By analyzing the level of Bax and Bim, we determined the Mcl-1/Bim, Bcl-x_L/Bax, Bcl-2/Bax and Bcl-2/Bim ratios. Our results indicate that Bcl-2/Bax and Bcl-2/Bim ratios predict the sensitivity of human melanoma cells to WFA-induced apoptosis. Such a correlation between a high Bcl-2/Bax ratio and resistance of human melanoma to apoptosis was previously observed in response to CD95/Fas [5], but not for Bcl-2/Bim. These proteins may thus function as important rheostats to determine the susceptibility of melanoma cells to WFA. Bcl-2 has been proposed to play a critical role in the mechanisms of resistance of melanoma since its overexpression reduces their sensitivity towards apoptotic stimuli [51]. Moreover, in human leukemia U937 cells, ectopic expression of Bcl-2 significantly attenuates WFA-induced apoptosis [20]. Here, we found that in human melanoma cells, overexpression of Bcl-2 only slightly reduced mitochondrial events of apoptosis promoted by WFA. We also discovered that WFA treatment provoked a marked decrease in Bcl-2 expression

level. These results demonstrate that even in a context of high Bcl-2 expression, WFA is able to kill human melanoma cells due, at least in part, to its capacity to down-regulate this anti-apoptotic protein. This latter property raises the potential usefulness of WFA for the treatment of malignant melanoma. Indeed, in different type of metastatic cancers, including melanoma, promising results were obtained with therapeutic strategies based on antisense oligonucleotides (e.g. oblimersen) that decrease Bcl-2 protein level. For instance, phase II and III trials conducted in patients with metastatic melanoma showed that treatment with Oblimersen alone or in combination with dacarbazine improves the clinical response [52, 53].

In conclusion, we demonstrated that very low doses of WFA induce apoptosis of human melanoma cells mainly by triggering ROS production, Bcl-2 down-regulation. This natural compound thus shows potential for the treatment of metastatic melanoma since it exhibits two pharmacological properties of other molecules used in clinical trials, i.e. a prooxidant activity (e.g. Disulfiram) and an ability to regulate Bcl-2 level (e.g. Oblimersen). Interestingly, the demonstration that WFA reduces tumor growth of human pancreatic [27] or breast cancer cells [25] in vivo, suggests that this compound could also be effective against malignant metastatic melanoma. More importantly, no noticeable toxicity of WFA was observed neither in human normal colon epithelial cells [23] nor in human lymphocytes [19], suggesting a specificity of WFA for cancer cells rather than for normal cells. However, further studies are required to validate our in vitro findings in an in vivo xenograft model of chemoresistant melanoma before embarking on human studies.

Acknowledgments We thank P. Lechene and D. Clay for their methodological help with fluorescence microscopy and flow cytometry platform at Institute André Lwoff, respectively. C. Longin from the microscopy and imagery platform of INRA is acknowledged. The compound LY335979 is a generous gift from Dr. M. Guttmann (Cytomics Pharmaceuticals). CB is supported by Institut National pour le Cancer (INCa, 2008-1-PL BIO-04-CNRS ON1) and Agence Nationale pour la Recherche (ANR, ANR-08PCVI-0008-01). CB, AL, LL, DD and CL are supported by the PRES UniverSud Paris (grant Peau et Biothérapie and grant for flow cytometry platform). EM, CG, and CM received fellowships from the Ministère de l'Enseignement Supérieur et de la Recherche (MESR).

Conflict of interest The authors declare that they have no conflict of interest.

References

1. Markovic SN, Erickson LA, Rao RD et al (2007) Malignant melanoma in the 21st century, part 2: staging, prognosis, and treatment. Mayo Clin Proc 82:490–513
2. Bhatia S, Tykodi SS, Thompson JA (2009) Treatment of metastatic melanoma: an overview. Oncology (Williston Park) 23:488–496
3. Lorigan P, Eisen T, Hauschild A (2008) Systemic therapy for metastatic malignant melanoma—from deeply disappointing to bright future? Exp Dermatol 17:383–394
4. Eberle J, Hossini AM (2008) Expression and function of bcl-2 proteins in melanoma. Curr Genom 9:409–419
5. Raisova M, Hossini AM, Eberle J et al (2001) The Bax/Bcl-2 ratio determines the susceptibility of human melanoma cells to CD95/Fas-mediated apoptosis. J Invest Dermatol 117:333–340
6. Hanahan D, Weinberg RA (2000) The hallmarks of cancer. Cell 100:57–70
7. Reed JC (2002) Apoptosis-based therapies. Nat Rev Drug Discov 1:111–121
8. Fulda S, Galluzzi L, Kroemer G (2010) Targeting mitochondria for cancer therapy. Nat Rev Drug Discov 9:447–464
9. Kroemer G, Galluzzi L, Vandenabeele P et al (2009) Classification of cell death: recommendations of the Nomenclature Committee on Cell Death 2009. Cell Death Differ 16:3–11
10. Kroemer G, Galluzzi L, Brenner C (2007) Mitochondrial membrane permeabilization in cell death. Physiol Rev 87:99–163
11. Chipuk JE, Fisher JC, Dillon CP, Kriwacki RW, Kuwana T, Green DR (2008) Mechanism of apoptosis induction by inhibition of the anti-apoptotic BCL-2 proteins. Proc Natl Acad Sci USA 105:20327–20332
12. Le Bras M, Clement MV, Pervaiz S, Brenner C (2005) Reactive oxygen species and the mitochondrial signaling pathway of cell death. Histol Histopathol 20:205–219
13. Fruehauf JP, Meyskens FL Jr (2007) Reactive oxygen species: a breath of life or death? Clin Cancer Res 13:789–794
14. Meyskens FL Jr, Farmer P, Fruehauf JP (2001) Redox regulation in human melanocytes and melanoma. Pigment Cell Res 14:148–154
15. Meyskens FL Jr, McNulty SE, Buckmeier JA et al (2001) Aberrant redox regulation in human metastatic melanoma cells compared to normal melanocytes. Free Radic Biol Med 31:799–808
16. Meyskens FL Jr, Buckmeier JA, McNulty SE, Tohidian NB (1999) Activation of nuclear factor-kappa B in human metastatic melanomacells and the effect of oxidative stress. Clin Cancer Res 5:1197–1202
17. Scartezzini P, Speroni E (2000) Review on some plants of Indian traditional medicine with antioxidant activity. J Ethnopharmacol 71:23–43
18. Malik F, Kumar A, Bhushan S et al (2007) Reactive oxygen species generation and mitochondrial dysfunction in the apoptotic cell death of human myeloid leukemia HL-60 cells by a dietary compound withaferin A with concomitant protection by N-acetyl cysteine. Apoptosis 12:2115–2133
19. Mandal C, Dutta A, Mallick A et al (2008) Withaferin A induces apoptosis by activating p38 mitogen-activated protein kinase signaling cascade in leukemic cells of lymphoid and myeloid origin through mitochondrial death cascade. Apoptosis 13:1450–1464
20. Oh JH, Lee TJ, Kim SH et al (2008) Induction of apoptosis by withaferin A in human leukemia U937 cells through down-regulation of Akt phosphorylation. Apoptosis 13:1494–1504
21. Srinivasan S, Ranga RS, Burikhanov R, Han SS, Chendil D (2007) Par-4-dependent apoptosis by the dietary compound withaferin A in prostate cancer cells. Cancer Res 67:246–253
22. Yang H, Shi G, Dou QP (2007) The tumor proteasome is a primary target for the natural anticancer compound Withaferin A isolated from "Indian winter cherry". Mol Pharmacol 71:426–437

23. Koduru S, Kumar R, Srinivasan S, Evers MB, Damodaran C (2010) Notch-1 inhibition by Withaferin-A: a therapeutic target against colon carcinogenesis. Mol Cancer Ther 9:202–210
24. Mohan R, Hammers HJ, Bargagna-Mohan P et al (2004) Withaferin A is a potent inhibitor of angiogenesis. Angiogenesis 7:115–122
25. Stan SD, Hahm ER, Warin R, Singh SV (2008) Withaferin A causes FOXO3a- and Bim-dependent apoptosis and inhibits growth of human breast cancer cells in vivo. Cancer Res 68:7661–7669
26. Kaileh M, Vanden Berghe W, Heyerick A et al (2007) Withaferin a strongly elicits IkappaB kinase beta hyperphosphorylation concomitant with potent inhibition of its kinase activity. J Biol Chem 282:4253–4264
27. Yu Y, Hamza A, Zhang T et al (2010) Withaferin A targets heat shock protein 90 in pancreatic cancer cells. Biochem Pharmacol 79:542–551
28. Lee TJ, Um HJ, Min do S, Park JW, Choi KS, Kwon TK (2009) Withaferin A sensitizes TRAIL-induced apoptosis through reactive oxygen species-mediated up-regulation of death receptor 5 and down-regulation of c-FLIP. Free Radic Biol Med 46:1639–1649
29. Deniaud A, Sharaf el dein O, Maillier E et al (2008) Endoplasmic reticulum stress induces calcium-dependent permeability transition, mitochondrial outer membrane permeabilization and apoptosis. Oncogene 27:285–299
30. Buron N, Porceddu M, Brabant M et al (2010) Use of human cancer cell lines mitochondria to explore the mechanisms of BH3 peptides and ABT-737-induced mitochondrial membrane permeabilization. PLoS ONE 5:e9924
31. Belzacq-Casagrande AS, Martel C, Pertuiset C, Borgne-Sanchez A, Jacotot E, Brenner C (2009) Pharmacological screening and enzymatic assays for apoptosis. Front Biosci 14:3550–3562
32. Guenal I, Sidoti-de Fraisse C, Gaumer S, Mignotte B (1997) Bcl-2 and Hsp27 act at different levels to suppress programmed cell death. Oncogene 15:347–360
33. Petronilli V, Miotto G, Canton M et al (1999) Transient and long-lasting openings of the mitochondrial permeability transition pore can be monitored directly in intact cells by changes in mitochondrial calcein fluorescence. Biophys J 76:725–734
34. Li P, Nijhawan D, Budihardjo I et al (1997) Cytochrome c and dATP-dependent formation of Apaf-1/caspase-9 complex initiates an apoptotic protease cascade. Cell 91:479–489
35. Clement MV, Pervaiz S (1999) Reactive oxygen intermediates regulate cellular response to apoptotic stimuli: an hypothesis. Free Radic Res 30:247–252
36. Circu ML, Aw TY (2010) Reactive oxygen species, cellular redox systems, and apoptosis. Free Radic Biol Med 48:749–762
37. Robinson KM, Janes MS, Pehar M et al (2006) Selective fluorescent imaging of superoxide in vivo using ethidium-based probes. Proc Natl Acad Sci USA 103:15038–15043
38. Hirpara JL, Clement MV, Pervaiz S (2001) Intracellular acidification triggered by mitochondrial-derived hydrogen peroxide is an effector mechanism for drug-induced apoptosis in tumor cells. J Biol Chem 276:514–521
39. Deneke SM (2000) Thiol-based antioxidants. Curr Top Cell Regul 36:151–180
40. Franco R, DeHaven WI, Sifre MI, Bortner CD, Cidlowski JA (2008) Glutathione depletion and disruption of intracellular ionic homeostasis regulate lymphoid cell apoptosis. J Biol Chem 283:36071–36087
41. Kamencic H, Lyon A, Paterson PG, Juurlink BH (2000) Monochlorobimane fluorometric method to measure tissue glutathione. Anal Biochem 286:35–37
42. La Porta CA (2007) Drug resistance in melanoma: new perspectives. Curr Med Chem 14:387–391
43. Dantzig AH, Shepard RL, Cao J et al (1996) Reversal of P-glycoprotein-mediated multidrug resistance by a potent cyclopropyldibenzosuberane modulator, LY335979. Cancer Res 56:4171–4179
44. Selzer E, Schlagbauer-Wadl H, Okamoto I, Pehamberger H, Potter R, Jansen B (1998) Expression of Bcl-2 family members in human melanocytes, in melanoma metastases and in melanoma cell lines. Melanoma Res 8:197–203
45. Bedard K, Krause KH (2007) The NOX family of ROS-generating NADPH oxidases: physiology and pathophysiology. Physiol Rev 87:245–313
46. St-Pierre J, Buckingham JA, Roebuck SJ, Brand MD (2002) Topology of superoxide production from different sites in the mitochondrial electron transport chain. J Biol Chem 277: 44784–44790
47. Vieira H, Kroemer G (2003) Mitochondria as targets of apoptosis regulation by nitric oxide. IUBMB Life 55:613–616
48. Fruehauf JP, Trapp V (2008) Reactive oxygen species: an Achilles' heel of melanoma? Expert Rev Anticancer Ther 8:1751–1757
49. Marengo B, De Ciucis C, Verzola D et al (2008) Mechanisms of BSO (L-buthionine-S,R-sulfoximine)-induced cytotoxic effects in neuroblastoma. Free Radic Biol Med 44:474–482
50. Gomez-Bougie P, Bataille R, Amiot M (2004) The imbalance between Bim and Mcl-1 expression controls the survival of human myeloma cells. Eur J Immunol 34:3156–3164
51. Raisova M, Goltz G, Bektas M et al (2002) Bcl-2 overexpression prevents apoptosis induced by ceramidase inhibitors in malignant melanoma and HaCaT keratinocytes. FEBS Lett 516:47–52
52. Bedikian AY, Millward M, Pehamberger H et al (2006) Bcl-2 antisense (oblimersen sodium) plus dacarbazine in patients with advanced melanoma: the Oblimersen Melanoma Study Group. J Clin Oncol 24:4738–4745
53. Jansen B, Wacheck V, Heere-Ress E et al (2000) Chemosensitisation of malignant melanoma by BCL2 antisense therapy. Lancet 356:1728–1733